J Fluoresc (2011) 21:179–186
DOI 10.1007/s10895-010-0702-5

ORIGINAL PAPER

A Sandwiched Biological Fluorescent Probe for the Diagnosis of Human Ovarian Tumor Based on TiO_2 Nanoparticles

Peisi Zhu · Shasheng Huang · Mengyao Li · Na Ding · Bing Peng · Lingmi Kong · Yang Bo

Received: 11 May 2010 / Accepted: 25 June 2010 / Published online: 6 July 2010

Abstract In this paper, we report a novel biological fluorescent probe for the diagnosis of human ovarian tumor based on sandwiched TiO_2 nanoparticles. The fluorescence nanoparticles consist of a fluorescent molecule, tetramethyl rhodamine isothiocyanate (TRITC), sandwiched between titanium dioxide (TiO_2) nanoparticles and nano-gold via reacting with each other. The antibodies HER2, labeled on the surface of the biofluorescence nanoparticles, have granted nanoparticles the privilege of aiming at peculiar tumor antigen. The specificity of antibody-nanoparticles interacting with cells was characterized by Laser Scanning Confocal Microscope. The results showed that these sandwiched nanoparticles were innocuous and stable, and the method offered potential advantages of sensitivity and simplicity due to high combing efficiency between nanoparticles and cells and provided an alternative method for the diagnosis of human ovarian tumor (HOT).

Keywords Nanometer titanium dioxide · Novelty nanosize fluorescence · Biological innocuity · Human ovarian tumor

Introduction

Cell recognition plays an important role in the biology and medicine and can be used for the disease diagnose and cell biology studies. Nanoparticles, with high reactivity, beneficial physical properties and ultrasmall size, are alternative materials used to get biological information inside or outside of a living specimen and provide an excellent analytical system for cell biology and immunoassay. Many successful examples of biocompatible nanoparticles have been introduced. The most nanoparticles used in this case are the nanoparticles doped with inorganic or organic dyes. For example, core-shell fluorescence nanoparticles encapsulating fluorescent dyes, such as the inorganic dye [tris (2,2′-bipyridyl) dichlororuthenium(II) hexahydrate] [1, 2], have been widely studied in fluorescent labeling of biomolecules and issue because their fluorescence characteristics are protected due to the high insulation from environment [3].

Nanometer titanium dioxide (TiO_2), a kind of n-semiconductor, has been used in the environmental field due to its excellent photocatalytic activity for some organic substances [4–6]. When irradiated by ultraviolet light at 387.5 nm, titanium dioxide nanoparticles (TiO_2 NPs) are excited, and the electron jumped from valence band to conduction band, producing free electron, electropositive hole and electron-hole pair (e-h+). TiO_2 NPs react with O_2 and OH^- adsorbed on the surface of these NPs to obtain free radical $\cdot O_2$ and hydroxyl free radical ·OH. Because these two free radicals can directly attack the cell wall, cell membrane and the intracellular constitutes of bacillus, the TiO_2 NPs has shown a strong power of killing pseudomonas aeruginosa, escherichia coli, staphylococcus, salmonella, cancel cell and so on [7]. The photocatalysis of TiO_2 to kill the cancel cell effectively offers a new way to cancer therapy. TiO_2 NPs, with great potential value in many fields such as biochemical immune because of their photo-

P. Zhu · S. Huang (✉) · M. Li · N. Ding · B. Peng · L. Kong · Y. Bo
College of Life and Environment, Shanghai Normal University, Shanghai 200234, China
e-mail: sshuang@shnu.edu.cn

catalysis, high stability, small size effect, surface effect and unique innocuity, have been received great attention of chemists and biologists.

As an excellent photocatalyst for some organic substances, the photoabsorption characteristics of the TiO_2 NPs can be changed by chemically modification. So far as we know, the most studies of titan dioxide are mainly focused on its photocatalysis [8]. However, there are few reports on its application in biological system, especially on the preparation and application of sandwiched TiO_2 nanoparticles. Gheshlaghi et al [9] reported the toxicity and interaction of titanium dioxide nanoparticles with microtubule protein. Their research showed that TiO_2 NPs have an inhibitory effect on microtubule protein. In the present work, we report a novel biological fluorescent probe based on a sandwiched model nanoparticles for the diagnosis of human ovarian tumor. The TiO_2 nanoparticles were prepared by the method of Sol-Gel. A common fluorescein, tetramethyl rhodamine isothiocyanate (TRITC), was sandwiched between TiO_2 and gold nanoparticles. The nanoparticles were clearly characterized by laser scanning confocal microscopy, scanning electron microscope and atomic force microscope. The toxicity of the fluorescein was weakened and optics stability of the nanoparticles did not changed due to the special sandwich construction. The results demonstrated that the fluorescent nanoparticles, as labels in tumor cell, showed a great improvement in sensitivity, selectivity.

Materials and methods

Chemicals

Tetrabutyl titanate, sodium borohydride, ethanol, sodium citrate, nitric acid and chloroauric acid were obtained from Sinopham Chemical Reagent Co., Ltd (Shanghai, China). 3-(4,5-dimethyl-thiazol-yl)-2,5-diphenyltetrazolium bromide (MTT), McCoy'5amedium and trypsinase were obtained from Sigma-Aldrich (St Louis, MO, USA). Fetal bovine serum was purchased from HyClone (FBS, Utah, USA). Penicillin, streptomycin, tetramethyl rhodamine isothiocyanate (TRITC), and sodium dodecyl sulfate (SDS) were obtained from Shanghai Sangon Biological Reagent Company (Shanghai, China). The SKOV-3 cell line was supplied by Shanghai Cell Bank (Shanghai, China). Monoclonal anti-HER2 antibodies from Chemicon International Inc (Temecula CA, USA) and the mouse anti-CEA from Zymed Laboratories (USA) were used in this experiment. Other chemical reagents used in the experiment were of analytical grade. Milli Q 18.3M_ water was used throughout the experiments.

Instruments

Fluorescence spectra were obtained using a Hitachi F-2500 luminescence spectrometer (Japan). The pictures of fluorescent nanoparticles were taken with a JEM-2100 transmission electron microscopy (TEM, JEOL, Japan) or atomic force microscopy (AFM, Veeco nano III a Multimode, USA). The results of the incubation of nanoparticles and cells were characterized with a laser scanning microscopy (Carl Zeiss, LSM 5 Pascal Laser Module, Germany). The MTT measurement was carried out using a spectrophotometer (Bio-RAD Model 680, USA). All optical measurements were carried out at room temperature under ambient conditions.

Synthesis of titanium dioxide NPs

Titanium dioxide NPs (TiO_2 NPs) were synthesized according to the method described by Li et al [5]. First, tetrabutyl titanate was put into 40 mL ethanol in the beaker with stirring under the 40°C water bath. Then a mixture solution containing 10 mL ethanol mixed with 2.5 mL nitric acid (V_{H2O}:V_{HNO3}=5:1) was added into above reactor beaker drop by drop with stirring until it became to pale yellow sol. The mixture solution was put into Drying Ovens (80°C) for 2 days to get titanium dioxide NPs powder. The titanium dioxide NPs was transferred into furnace for 4 h at 500°C prior to abrade it in the agate mortar.

Synthesis of AuNPs

Au colloid (AuNPs) was prepared according to the literature [10]. All the glassware used in the following procedure was cleaned in a bath of freshly prepared solution of aqua regia for about 30 min, and rinsed thoroughly with pure water and then dried in air. 50 mL 0.01% $HAuCl_4$ was heated to a boiling condition with vigorous stirring, then 1.75 mL 1% sodium citrate was rapidly added, which resulted in a color change from pale yellow to blue, and finally arrived at red–violet. The solution of Au colloidal particles was examined by UV–vis spectra. The result showed a strong peak at 525 nm due to their surface plasma resonance, the characteristics of monodisperse colloidal Au [10, 11].

Conjunction of fluorescent nanotitan dioxide and AuNPs

Dissolve 0.01 g tetramethyl rhodamine isothiocyanate (TRITC) in the ultra-pure water (3.63 mL), after 0.2 g TiO_2 nanopowder was added, the mixture was stirred for 3 days prior to air it at room temperature. The TiO_2-TRITC-Au powder can be obtained by mixture 0.1069 g TRITC-TiO_2 and 1,855 μL AuNPs. Figure 1 illustrates schematic

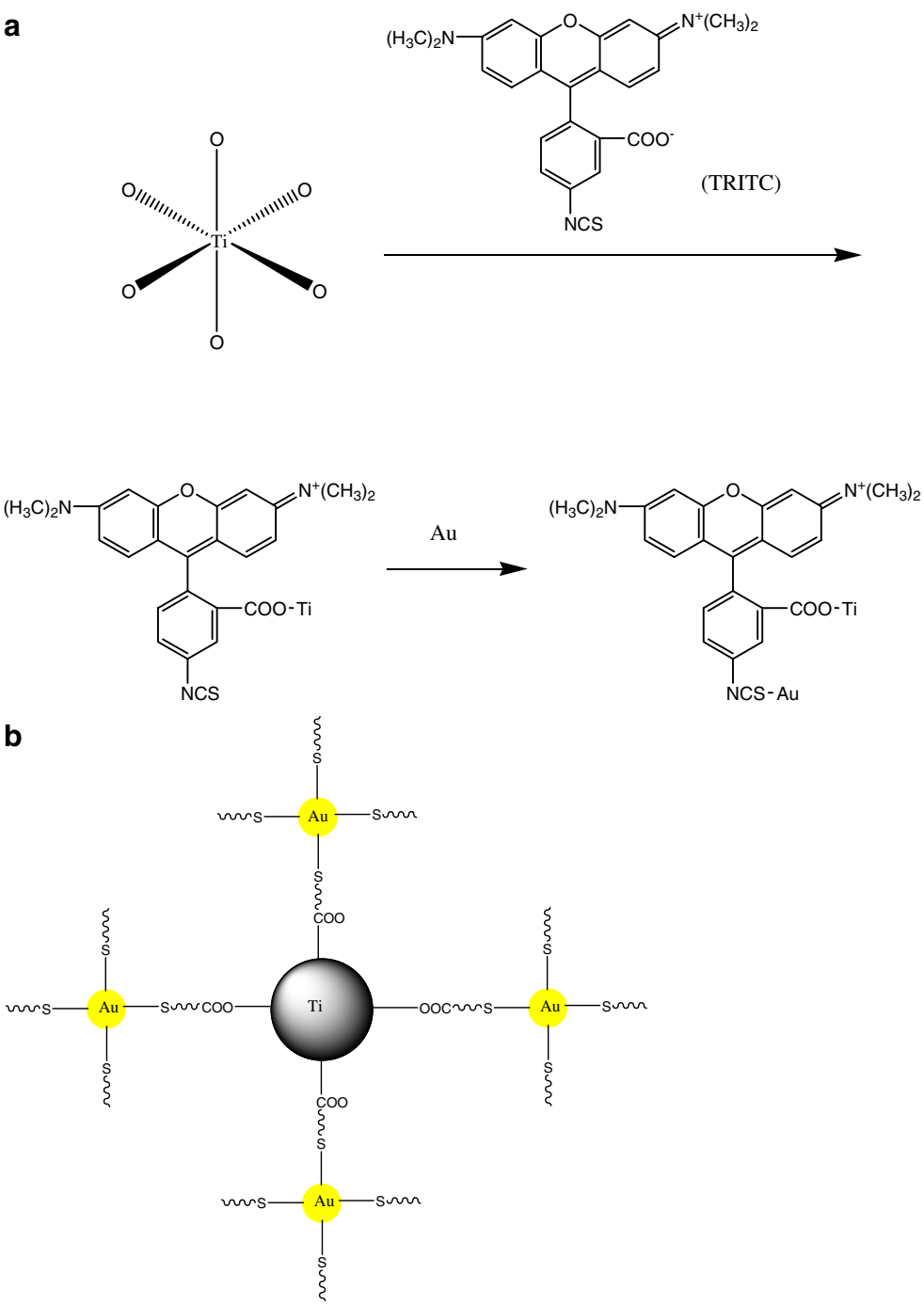

Fig. 1 Schematic of synthesis of fluorescent nanoparticles: **a** the synthesize process of the novelty material; **b** the possible structure of the novelty material

of the synthesis process and possible structure of resulting fluorescence nanoparticles consisted of a fluorescent molecule, tetramethyl rhodamine isothiocyanate (TRITC), sandwiched between titanium dioxide (TiO_2) nanoparticles and nano-gold. In this paper, TiO_2- TRITC- Au NPs was used to denote above nanoparticles.

The immobilization of anti-HER2 on the TiO_2- TRITC-Au NPs was achieved by adding 25 μL anti-HER2 into the aqueous solution containing TiO_2-TRITC- Au NPs, stirring and mixing them in the refrigerator (4°C).

Cell culture and incubation of nanoparticles bioconjugates with cells

SKOV-3 cell line were grown on glass cover slips in McCoy'5a medium supplemented with 10% FBS, 100 units/mL of penicillin, and 100 μg/mL of streptomycin in an atmosphere of 95% humidified air and 5% CO_2 at 37°C. Cells were cultured until exponential phase, the growth medium was replaced by a fresh McCoy'5a medium supplemented with 25 μL nanoparticles connected by anti-HER2 or 25 μL

with FITC connected by anti-CEA, shaken up, and incubated at 37°C for 2 h, and characterized by the LSM.

Cell viability experiment

The cells were trypsinized with trypsinase and suspended in McCoy'5a medium at a concentration of 10^4~10^5 cells/mL. Then an amount of 10^3~10^4 cells/well (100 μL) was seeded in 96-well culture plate and allowed it to adhere overnight in an incubator at 37°C with 5% CO_2. Media was exchanged with fresh medium containing varying concentration fluorescent nanoparticles (10 μL aqueous dispersion per well) and mixed gently. The plates were then set for 44 h, and then 20 μL of MTT dissolved in physiological brine at 5 mg/mL was added to each well. After the cells were incubated for 4 h again, 100 μL SDS was added to each well and incubated continuously for another 12 h in order to dissolve any purple MTT formazan crystals at room temperature. Finally, the absorbance was measured by ELIASA.

Results and discussion

Characterization of fluorescent nanoparticles

Figure 2 shows the transmission electron micrographs (TEM) of the TiO_2 NPs (Fig. 2a) and Au NPs (Fig. 2b). As can be seen from the Fig. 2, the nanoparticles are dispersed well, and the diameters of the nanoparticles for titanium dioxide and Au NPs were ca 25 nm and ca 8 nm, respectively. It was found that the nanoparticles newly prepared have much bigger size.

XPS of the nanoparticles

To have an in-depth understanding of the structure of the nanoparticles, the composition of the sandwiched fluorescence nanoparticles was investigated. Figure 3 displays the XPS spectra of elements participated in the synthesis of fluorescent nanoparticles, curves a and b in Fig. 3 are the spectra obtained by Au/TiO_2 and TiO_2-Au-TRITC NPs, respectively. As shown in Fig. 3a, the binding energy of Ti $2p_{3/2}$ is equal to 461.2 eV and the binding energy of Ti $2p_{1/2}$ is equal to 467 eV. Both Yang et al [12] and Herman [13] reported that the binding energies of Ti $2p_{3/2}$ and Ti $2p_{1/2}$ were 458.5 eV and 464.1 eV, respectively. Compared with the results obtained by these reports, the peaks of Ti $2p_{3/2}$ and Ti $2p_{1/2}$ here shifted ca 2 eV. The reason producing this phenomenon maybe due to the existence of a large amount of surfactants during synthesis of the nanoparticles, which not only induces the congregation of electrons on the TiO_2 surface, but also induces the orbit of Ti orbit to be changed. On the other hand, there are some differences between hollow TiO_2 nanoparticles prepared by Yang et al [12] and the TiO_2 nanoparticles synthesized here.

The XPS peaks of Au $4f_{5/2}$ and $4f_{7/2}$ (Fig. 3b) for the nanosized metallic Au at 87.3 and 83.7 eV with a separation of spin-orbit coupling of 3.6 eV can be clearly observed for the freshly prepared sample Au nanoparticles. The data are in reasonable agreement with those reported in the literature [14]. But for the Au-TRITC-TiO_2 particles, the separation of spin-orbit coupling decreased to 1.2 eV, which related to the change of Au particle size [15–17].

The O_{1s} XPS spectra are exhibited in Fig. 3c. The peak at 533 eV, coincident with those reported in the literature (529.5 eV) [14], can be assigned to oxygen specie in H_2O molecules and Ti-OH or CO_3^{2-} [14, 18]. A higher binding energy of the Ti 2p measured at 461.2 and 467 eV can be ascribed to a higher degree of charge transfer from Ti cations to carboxyl in the sample.

The peaks for S_{2s} are shown in Fig. 4; the peak at 231.2 eV can be assigned to the S-Au bond. Clearly, thiol ends from TRITC molecules can contribute to the S-Au formation [19]. This result is rather expected since all organic sulfur is reacted with the Au nanoparticles easily.

Possible structure of novelty fluorescent nanoparticles

Figure 1 illustrates the synthesis process and possible structure of the TRITC-doped TiO_2 and Au fluorescent nanoparticles in this paper. According to the synthesis

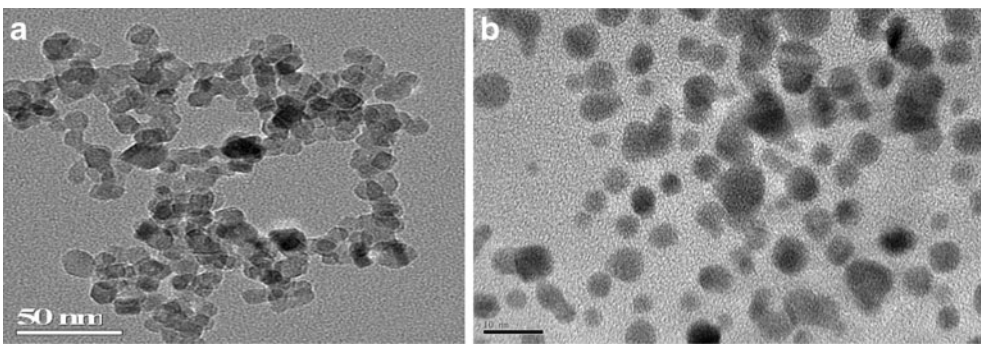

Fig. 2 TEM image of TiO_2 NPs (**a**) and Au NPs (**b**)

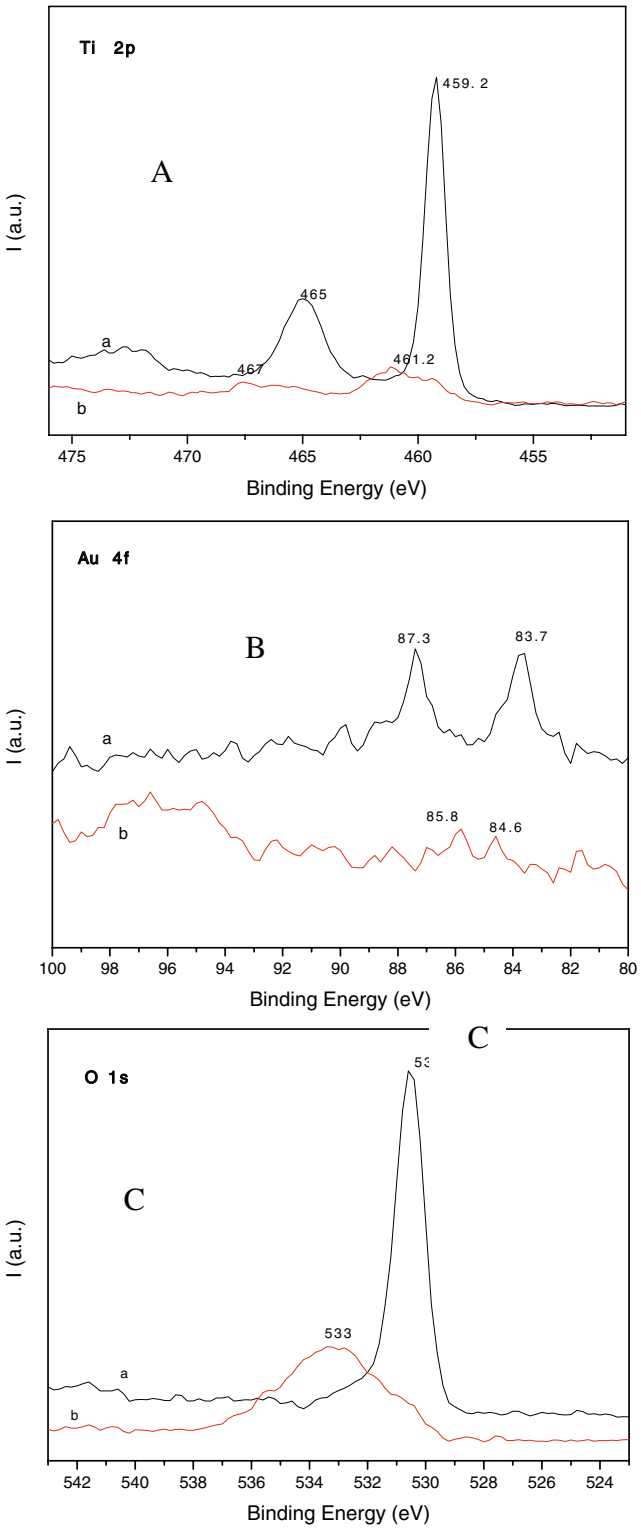

Fig. 3 **a** XPS spectra of Ti 2p; **b** XPS spectra of Au 4f; **c** XPS spectra of O 1 s. **a** as-prepared Au/TiO_2, **b** Au-TRITC-TiO_2

process of the nanoparticles, we speculate that the network is formed (Fig. 1b). This sandwich network maybe stable due to sandwich structure. We supposed the formation process of the sandwich nanoparticles as follows: At first,

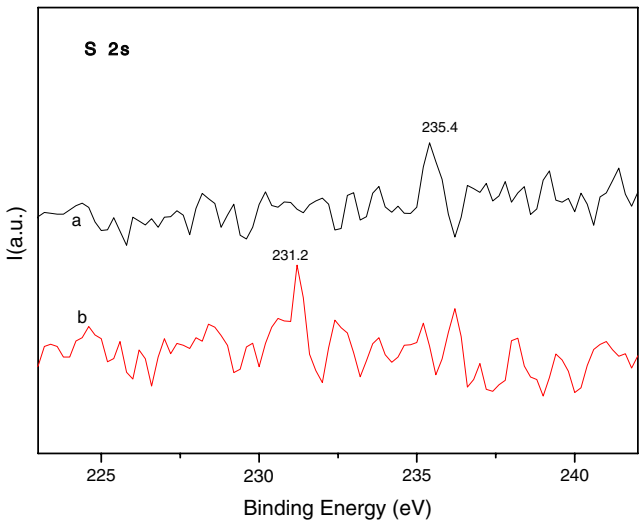

Fig. 4 XPS spectra of S_{2s}

TRITC with carboxyl group was connected onto the surface of TiO_2 [20–22], and then assigned to the gold through S-Au bond as reported in the literature [23–25]. When the functional group is reacting with each other, the uniform and stable fluorescent nanoparticles can be obtained due to the presence of bifunctional groups in the TRITC linker molecules [14]. Figure 5 shows the AFM images of the sandwiched fluorescent nanoparticles. From Fig. 5, the morphology of the nanoparticles can be seen clearly.

Photobleaching experiment

In the biological detection system, the photostability of the fluorescent nanoparticles is very important. TRITC is an organic dye and is extensively used as a label in the bio-analysis. But the photostability of TRITC is rather poor. The photobleaching experiments of TRITC and the nanoparticles were carried out at an excitation wavelength of 558 nm (Fig. 6). As shown in Fig. 6, over 400 min of successively irradiation, the fluorescence intensity of the TiO_2 - TRITC-Au NPs did not decrease obviously. However, for the pure TRITC, the fluorescence intensity decreased quickly and significantly after exposing under the excitation light. The result demonstrated that the photostability of the fluorescent nanoparticles was much better than that of the pure TRTIC, indicating that the fluorescent nanoparticles were more photostable due to the sandwiched structure and the photo-stability of the fluorescent nanoparticles prepared here was similar to the core -shell nanoparticles [26, 27].

Fluorescent image in the conjunction of cell and nanoparticles

The target cell recognition could be helpful in biochemical analysis and clinical diagnosis. Human ovarian carcinoma

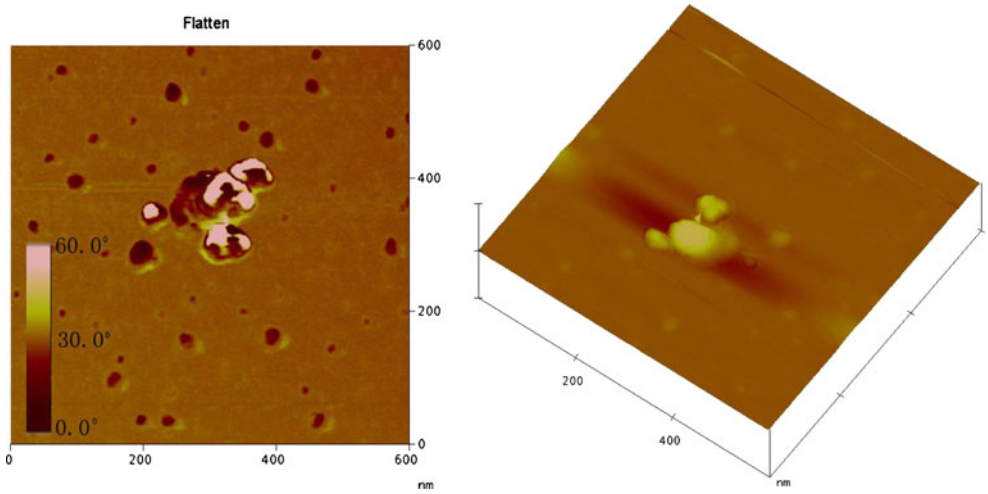

Fig. 5 AFM characterizations of TiO_2- TRITC –Au NPs

cells SKOV-3 [28] are HER2— overexpressing tumor cells. The antigen of this tumor cell can be selectively targeted using anti-HER2 monoclonal antibody easily. Huang et al [29] synthesized shell-core SiO2 fluorescent nanoparticles for the detect of cells SKOV-3. Here, we used TiO_2-TRITC-Au NPs as a biological label for recognizing target cells, human ovarian carcinoma (SKOV-3). First, luminescent TiO_2-TRITC-Au NPs were covalently immobilized with anti-HER2 according to the procedure described prior. The incubated cells were imaged with both optical and fluorescence microscopy. Figure 7 a shows the optical image. As shown in Fig. 7b, after the SKOV-3 cells were incubated with TiO_2-TRITC-Au NPs modified anti- HER2, the bright emission of some cells could be observed by Laser scanning microscopy. The optical image of the cells correlated well with the fluorescence image. In contrast, the control experiment with bare luminescent TiO_2-TRITC-Au did not show any fluorescence signal of the cells. From Fig. 7, it can be seen that the cells with bright emission

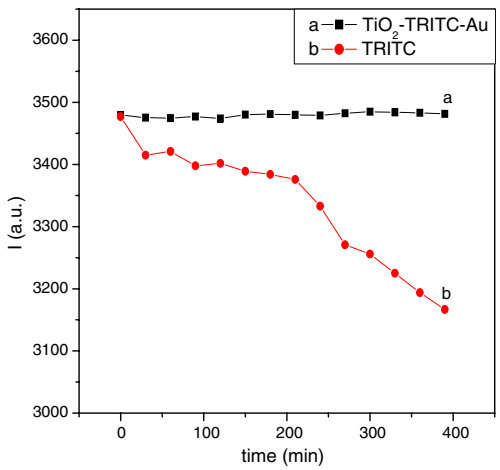

Fig. 6 Photostability of TiO_2-TRITC-Au NPs (**a**) and TRITC in the solution (**b**)

under fluorescence microscopy are SKOV-3. These cells were recognized selectively by the TiO_2-TRITC-Au NPs labeled with anti-HER2. The antibodies were caught by the network of the materials and took place immunoreaction with the antigens in the surface membrane of the SKOV-3 cells. For the non-special antibody, anti-CEA, the cells are not connected with this antibody (Fig. 7c), indicating that there is a specific immunoreaction between the SKOV-3 by anti-HER2.

Activity analysis of SKOV-3 cell with novelty fluorescent nanoparticles

The anti-HER2-NPs can combine with the antigen in the cell easily because SKOV-3 cell is an over-expressing HER2 human ovarian carcinoma cells. In this paper, the colorimetric MTT assay was used to measure the cell proliferation and viability according to the literature [30–33]. In the MTT assay, the absorbance of formazan produced by the MTT cleavage caused by dehydrogenases in living cells at 570 nm reflects the amount of alive cells. The spectrophotometer was calibrated to zero absorbance using culture medium without cells. The sample without nanoparticles was taken as a control group, and the absorbance of the sample containing TiO_2-TRITC-Au NPs was measured. We can adopt following expression to calculate the inhibitory rate (%) [34]:

$$\text{Inhibitory rate} = \left(\left([\text{A}]_{\text{control}} - [\text{A}]_{\text{test}}\right)/[\text{A}]_{\text{control}}\right) \times 100\%$$

where $[\text{A}]_{\text{control}}$ is the absorbance of control sample; and $[\text{A}]_{\text{test}}$ is the absorbance of nanoparticles-exposed cells.

The lower the cell growth inhibitory rate obtained is, the lower toxicity of the nanoparticles is. Figure 8 shows the MTT assay results of the culture of nanoparticles and cells.

From Fig. 8, it can be found that the cell growth inhibitory rate was close to zero when adding 1×10^{-3} g/mL

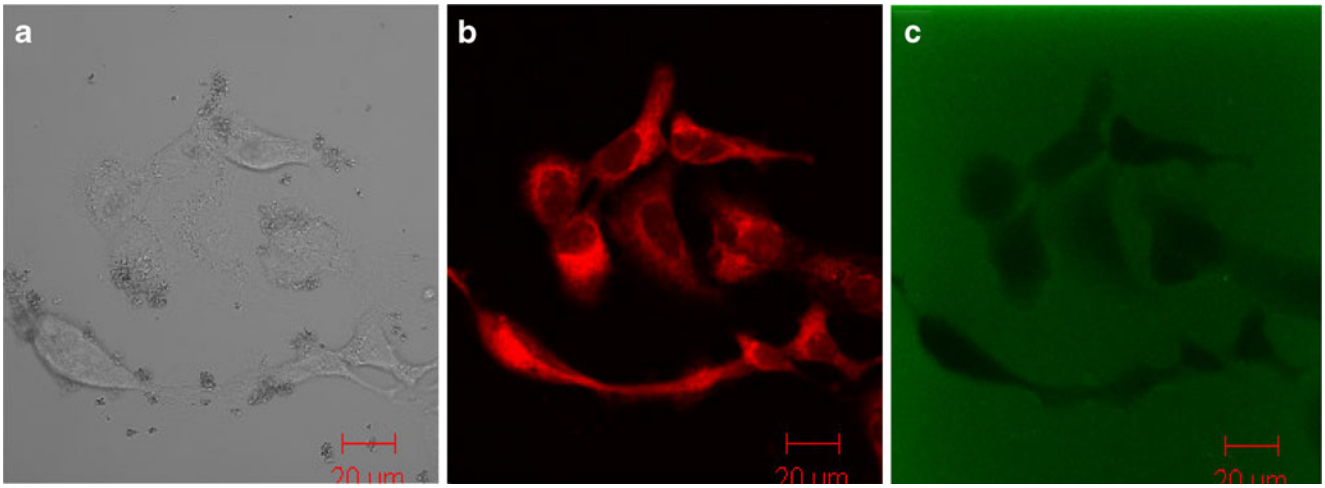

Fig. 7 Optical images (**a**) and fluorescence image of KOV-3 incubated with anti- HER2 - TiO_2- TRITC –Au NPs (**b**); fluorescence image of SKOV-3 incubated with anti- CEA - TiO_2- TRITC –Au NPs (**c**)

of TiO_2-TRITC-Au nanoparticles to culture cell, indicating that biofluorescent nanoparticles showed very low or no toxicity on the cells. In contrast to TiO_2-TRITC-Au NPs, when TRITC with same concentration as nanoparticles was used, the relative cell growth inhibitory rate of 70.82% showed that the pure TRITC greatly killed all the cells and the toxicity of TiO_2-TRITC-Au NPs was much lower than that of pure TRITC in this case. It is interesting that when none of nanoparticles were added into cells, a negative value of inhibitory rate was obtained. Perhaps the nanoparticles were metabolized as a foreigner by the cells. It seems that the effect of the nanoparticles is very complex and need to study in depth in further work. Obviously, the larger the addition concentration of nanoparticles was added, the more difficult the cell metabolism became, and the cell life activity and metabolism were affected obviously.

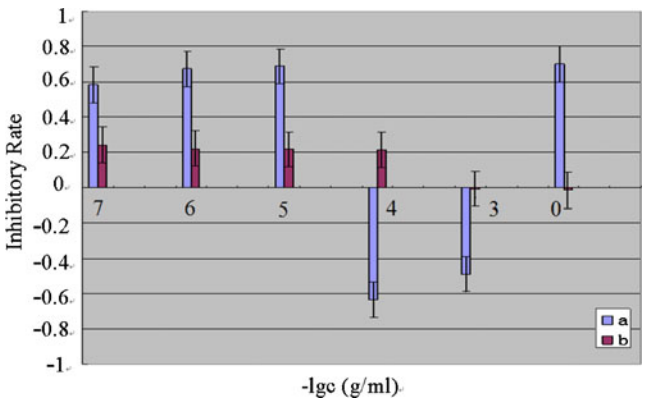

Fig. 8 Inhibitory rate of the cells by TRITC (**a**) and nanoparticles (**b**)

Conclusion

The antibody was easily immobilized on the surface of TiO_2-TRITC-Au nanoparticles with a sandwich structure. The TiO_2-TRITC-Au nanoparticles label has some unique advantages over the pure TRITC label in the photostability and toxicity. A stable compound formed after the nanoparticles cultured with SKOV-3 cells of coverexpressing HER2 antigen. The MTT experiment showed that the fluorescent nanoparticles had little cell toxicity to HOT cells. When the addition concentration of nanoparticles was 1×10^{-3} g/mL, the novelty nanoparticles are regarded as innocuity , which providing the foundation of the cell detection using fluorescent nanoparticles. This method provided an alternative method of determination of HOT. Our results indicate that the novel fluorescence probe based on TiO_2-TRITC-Au nanoparticles is potential biomarkers that would play important roles in cell recognition and other biochemical analysis. It is possible that different cancer cells can be detected by modification of different antibodies on the NPs.

This method, using the designed antibody-functionalized fluorescent nanoparticles specifically targets specific antigen on ovarian carcinoma cells SKOV-3 for realizing the aim of detecting tumor cells, can be used as a new measure technique in biological assay- antigen-antibody affinity assays.

Acknowledgment This work was supported by the National High-tech R&D program (863 program, 2007AA06Z402), Project of the Foundation of Shanghai Municipal Government (08520510400), Shanghai Leading Academic Discipline Project (S30406) and Key Laboratory of Resource Chemistry of Ministry of Education.

References

1. Tan WH, Santra S, Zhang P (2001) U.S. Patent 09/572, 469
2. Qhobosheane M, Santra S, Zhang P, Tan WH (2001) Biochemically functionalized silica nanoparticles. Analyst 126:1274–1278. doi:10.1039/b101489g
3. Zhao XJ, Tapec-Dytioco R, Tan WH (2003) Ultrasensitive DNA detection using highly fluorescent bioconjugated nanoparticles. J Am Chem Soc 125:11474–11475. doi:10.1021/ja0358854
4. Bian ZF, Zhu J, Cao FL, Lu YF, Li HX (2009) In situ encapsulation of Au nanoparticles in mesoporous core–shell TiO_2 microspheres with enhanced activity and durability. Chem Commun 25:3789–3791. doi:10.1039/b906825b
5. Li HX, Zhang XY, Huo YN, Zhu J (2007) Supercritical preparation of a highly active S-doped TiO_2 photocatalyst for methylene blue mineralization. Environ Sci Technol 41:4410–4414. doi:10.1021/es062680x
6. Wang JA, Limas-Ballesteros R, Lopez T, Moreno A, Gomez R, Novaro O, Bokhimi X (2001) Quantitative determination of titanium lattice defects and solid-state reaction mechanism in iron-doped TiO_2 photocatalysts. J Phys Chem B 105:9692–9698. doi:10.1021/jp0044429
7. Chen AL, Zhou F, Chen XY, Chen J (2005) Photochemical performance and research progress of nanometer titanium dioxide. Hunan Metallurgy 33:3–7
8. Ding Z, Lu GQ, Greenfield PF (2000) Role of the crystallite phase of TiO_2 in heterogeneous photocatalysis for phenol oxidation in water. J Phys Chem B 104:4815–4820. doi:10.1021/jp993819b
9. Gheshlaghi ZN, Riazi GH, Ahmadian S (2008) Toxicity and interaction of titanium dioxide nanoparticles with microtubule protein. Acta Biochim Biophys Sin 40:777–782. doi:10.1111/j.1745-7270
10. Brown KR, Walter DG, Natan MJ (2000) Seeding of colloidal Au nanoparticle solutions. 2. Improved control of particle size and shape. Chem Mat 12:306–313, 10.1111/j.1745-7270
11. Mao B, Liu B, Wang Y, Li GG, Sun YZ, Ma LP, Liu GH (2009) Preparation of Au colloid of small size in aqueous solution. Rare Metal Materials and Engineering 38:515–518
12. Yang HG, Zeng HC (2004) Preparation of hollow anatase TiO_2 nanospheres via ostwald ripening. J Phys Chem B 108:3492–3495. doi:10.1111/j.1745-7270
13. Herman GS, Gao Y (2001) Growth of epitaxial anatase (001) and (101) films. Thin Solid Films 397:157–161. doi:10.1016/S0040-6090(01)01476-6
14. Li J, Zeng HC (2006) Preparation of monodisperse Au/TiO_2 nanocatalysts via self-assembly. Chem Mater 18:4270–4277. doi:10.1021/cm060362r
15. Zhang L, Persaud R, Madey TE (1997) Ultrathin metal films on a metal oxide surface: growth of Au on TiO_2 (110). Phys Rev B 56:10549–10557. doi:10.1103/PhysRevB.56.10549
16. Chang FW, Yu HY, Roselin LS, Yang HC (2005) Production of hydrogen via partial oxidation of methanol over Au/TiO_2 catalysts. Appl Catal A 290:138–147. doi:10.1016/j.apcata.2005.05.024
17. Schumacher B, Plzak V, Kinne M, Behm R (2003) Highly active Au/TiO_2 catalysts for low-temperature CO oxidation: preparation, conditioning and stability. J Catal Lett 89:109–114
18. Chang Y, Lye ML, Zeng HC (2005) Large-scale synthesis of high-quality ultralong copper nanowires. Langmuir 21:3746–3748. doi:10.1021/la050220w
19. Nakamura T, Kimura R, Sakai H, Abe M, Kondoh H, Ohta T, Matsumoto M (2002) Nano-dot formation using self-assembled 3-mercaptopropionic acis thin film prepared by facile atmospheric-vapor-adsorption method on Au (111). Appl Surf Sci 202:241–251. doi:PII: S0169-4332(02)0947-9
20. Bates SP, Kresse G, Gillian MJ (1998) The adsorption and dissociation of ROH molecules on TiO_2 (110). Surf Sci 409:336–349
21. Käckell P (2000) First-principle analysis of the dissociative adsorption of formic acid on rutile TiO_2 (110). Appl Surf Sci 166:370–375. doi:10.1016/S0169-4332(00)00451-7
22. Käckell P, Terakura K (2000) Dissociative adsorption of formic acid and diffusion of firmate on the TiO_2 (110) surface: the role of hydrogen. Surf Sci 461:191–198
23. Lukkari J, Meretoja M, Kartio I, Laajalehto K, Rajamäki M, Lindström M, Kankare J (1999) Organic Thiosulfates (Bunte Salts): novel surface-active sulfur compounds for the preparation of self-assembled monolayers on gold. Langmuir 15:3529–3537. doi:10.1021/la9811719
24. Gonella G, Cavalleri O, Terreni S, Cvetko D, Floreano L, Morgante A, Canepa M, Rolandi R (2004) High resolution X-ray photoelectron spectroscopy of 3-mercaptopropionic acid self-assembled films. Surf Sci 566(568):638–643
25. Jiang L, Glidle A, McNeil CJ, Cooper JM (1997) Characterization of electron transfer reactions of microperoxidase assembled at short-chain thiol-monolayers on gold. Biosens Bioelectron 12:1143–1155. doi:PII: S0956-5663(97)00085-7
26. Wang CL, Zhang H, Zhang JH, Li MJ, Sun HZ, Yang B (2007) Application of ultrasonic irradiation in aqueous synthesis of highly fluorescent CdTe/CdS core-shell nanocrystals. J Phys Chem C 111:2465–2469. doi:10.1021/jp066601f
27. He XX, Wang KM, Li D, Tan WH, He CM, Huang SS, Liu B, Lin X, Chen XH (2003) A novel DNA-enrichment technology based on amino-modified functionalized silica nanoparticles. J Dispers Sci Technol 24:633–640
28. Lu JP, Sun H, Ou ZL (2003) Apoptosis of ovarian cancer cell line SKOV3 induced by arsenic trioxide. Prog Obstet Gynecol 12:93–95
29. Huang SS, Li RN, Qu YX, Shen J, Liu J (2009) Fluorescent biological label for recognizing human ovarian tumor cells based on fluorescent nanoparticles. J Fluoresc 19:1095–1101. doi:10.1007/s10895-009-0509-4
30. Ye ZQ, Tan MQ, Wang GL, Yuan JL (2005) Development of functionalized terbium fluorescent nanoparticles for antibody labeling and time-resolved fluoroimmunoassay application. Talanta 65:206–210. doi:10.1016/j.talanta.2004.06.008
31. Tarnuzzer RW, Colon PS, Seal S (2005) Vacancy engineered ceria nanostructures for protection from radiation-induced cellular damage. Nano Lett 5:2573–2577. doi:10.1021/nl052024f
32. Xu PS, Van Kirk EA, Murdoch WJ, Zhan YH, Isaak DD, Radosz M, Shen YQ (2006) Anticancer efficacies of cisplatin-releasing pH-responsive nanoparticles. Biomacromolecules 7:829–835. doi:10.1021/bm050924y
33. Xu PS, Van Kirk EA, Li SY, Murdoch WJ, Ren J, Hussain MD, Radosz M, Shen YQ (2006) Highly stable core-surface-crosslinked nanoparticles as cisplatin carriers for cancer chemotherapy. Colloids Surf B Biointerfaces 48:50–57. doi:10.1016/j.colsurfb.2006.01.004
34. Lin F, Lu QX, Lu L, Liang Y (2007) Inhibitory effect of extracts of digestive gland on proliferation of tumor cells. Carcinogensis, Teratogenesis and Mutagenesis 19:116–118